J. Fluid Mech. (1971), *vol.* 46, *part* 4, *pp.* 737–747
Printed in Great Britain

Jet flow instability of an inviscid compressible fluid

By WILLIAM BLUMEN
Department of Astro-Geophysics, University of Colorado, Boulder

(Received 1 September 1970)

A linear analysis of the perturbations associated with the jet flow, $\bar{u}(y) = \operatorname{sech} y$, of an inviscid compressible fluid is considered. Some subsonic stable solutions, not associated with stability boundaries, are first determined. Then a subsonic neutral solution is found and used as an aid in determining stability boundaries of the symmetric and antisymmetric disturbance modes. Numerical methods are also used to determine instability characteristics, including the Reynolds stress distributions. Comparisons are made with previous results obtained for the hyperbolic-tangent velocity profile and with unstable characteristics of the Bickley jet.

1. Introduction

Recently, an investigation of the stability of a compressible shear layer, represented by the hyperbolic-tangent profile, was presented (Blumen 1970). In this study, hereafter referred to as I, viscosity and heat conduction were omitted and the fluid medium was assumed to be an ideal gas, whose basic thermodynamic state is constant. This physical model is a relatively straight-forward extension of the homogeneous fluid model which defines the Rayleigh stability problem. The essential difference lies in the fact that perturbation pressure changes, associated with the compressibility of the medium, are possible. In the limit, as the fluid tends toward incompressibility (Mach number $M \to 0$), the Rayleigh stability equation governs fluid motions (see (4)).

The stability analysis in I was basically a numerical study abetted by a neutral solution of the stability equation (3). The investigation revealed that the compressibility of the medium is a stabilizing feature, at least for disturbances whose real phase speed is subsonic relative to the basic flow at infinity. Perhaps the most interesting feature uncovered was the appearance of a discontinuity in the slope of the Reynolds stress τ across the critical point, where the inflection in the velocity profile occurs. An initial second-order tendency toward the creation of a Kelvin–Helmholtz shear layer occurs as a by-product of this jump in $d\tau/dy$.

The present investigation is intended to complement the work in I, by considering the stability of a symmetric velocity profile. Since it was realized that reliance on numerical computations was a necessary adjunct, it seemed desirable to choose a velocity profile for which a neutral solution could be obtained and used to check numerical results. The ultimate decision was based on the virtues of the hyperbolic-secant profile and its square, the Bickley jet. Some recent calculations of the eigenvalues associated with the Bickley jet, for $M = 0$, have been displayed by Drazin & Howard (1966). However, the hyperbolic-secant profile was chosen

for this investigation because a neutral solution for $M = 1$ could be obtained. Moreover, a rich harvest of stable solutions, not associated with stability boundaries, could also be determined. Finally, it was felt that an investigation of the hyperbolic-secant profile would make a useful contribution to the library of solutions of the Rayleigh problem ($M = 0$), which have been documented by Drazin & Howard.

2. Basic equations

The model and attendant stability problem have been discussed in I. Briefly, we consider the linear stability of a basic plane parallel flow, $\bar{u}^*(y^*)$, of an ideal gas moving in the x^* direction with transverse variations in the y^* direction. Superposed on a basic thermodynamic state, characterized by a constant adiabatic sound speed $a^* \equiv \gamma \bar{p}^*/\bar{\rho}^*$, are (x^*, y^*) components of the perturbation velocity (u^*, v^*) and pressure p^*. The basic parameter of this model is the Mach number $M \equiv U/a^*$, where U is a characteristic velocity scale of the basic flow associated with its transverse variation over a length scale L. In the usual manner, we define non-dimensional co-ordinates, time, velocities and pressure as

$$\left.\begin{aligned} &(x, y) \equiv (x^*, y^*)/L, \quad t \equiv t^* U/L, \\ &\bar{u} \equiv \bar{u}^*/U, \quad (u, v) \equiv (u^*, v^*)/U, \\ &\pi \equiv p^*/\bar{\rho}^* U^2. \end{aligned}\right\} \tag{1}$$

We investigate the stability of the basic flow to normal mode disturbances.

$$q = \hat{q}(y) \exp[i\alpha(x - ct)], \tag{2}$$

where q is u, v or π, α is the real x wave-number and $c = c_r + ic_i$ is the complex phase velocity. Then, from I, the differential equations for the amplitudes of pressure $\hat{\pi}$ and velocity $\hat{v}$ are

$$(\bar{u} - c)\hat{\pi}'' - 2\bar{u}'\hat{\pi}' - \alpha^2(\bar{u} - c)[1 - M^2(\bar{u} - c)^2]\hat{\pi} = 0 \tag{3}$$

and

$$([(\bar{u} - c)\hat{v}' - \bar{u}'\hat{v}]/[1 - M^2(\bar{u} - c)^2])' - \alpha^2(\bar{u} - c)\hat{v} = 0, \tag{4}$$

where a prime denotes differentiation with respect to y. The relationships between the perturbation quantities may be expressed as

$$\left.\begin{aligned} \hat{v} &= i\alpha^{-1}(\bar{u} - c^*)\hat{\pi}'/|\bar{u} - c|^2, \\ \hat{u} &= -(\bar{u} - c^*)(\hat{\pi} - i\alpha^{-1}\bar{u}'\hat{v})/|\bar{u} - c|^2, \end{aligned}\right\} \tag{5}$$

where c^* is the complex conjugate of c.

For subsonic disturbances relative to the basic flow at infinity,

$$1 - M^2(\bar{u} - c)^2 > 0,$$

all perturbation amplitudes decay exponentially in the transverse direction. Accordingly,

$$\hat{v} = \hat{\pi} = 0 \quad (y = \pm\infty). \tag{6}$$

On rigid boundaries the normal velocity must vanish. From (5), the corresponding boundary conditions are

$$\hat{v} = \hat{\pi}' = 0 \quad (y = y_1, y_2). \tag{7}$$

3. Stable and neutrally stable waves

Stable waves

There are two classes of stable disturbances which are subsonic at infinity. One type is adjacent to unstable subsonic disturbances and is usually referred to as a 'neutral' subsonic disturbance. Lees & Lin (1946) established that a necessary and sufficient condition for the existence of a neutral subsonic disturbance is

$$\bar{u}'' = 0 \quad \text{at} \quad y = y_s, \tag{8}$$

where y_s is the point where $\bar{u} = c_r$. If the velocity profile is symmetric, there can be two inflection points where $\bar{u} = c_r$. We shall consider neutral waves associated with the hyperbolic-secant profile in due course. At present, we turn our attention to the second class of stable disturbances which apparently have remained untouched in the literature.

Upon division by $(\bar{u}-c)^3$, (3) may be written

$$([\bar{u}-c]^{-2}\hat{\pi}')' - \alpha^2([\bar{u}-c]^{-2} - M^2)\hat{\pi} = 0. \tag{9}$$

For the present, we let $c = c_r$ and assume $(u-c_r)^2 > 0$. Multiplication of (9) by $\hat{\pi}^*$, the complex conjugate of $\hat{\pi}$, and application of (6) and/or (7) yields

$$\int_{y_1}^{y_2} (\bar{u}-c_r)^{-2} |\hat{\pi}'|^2 dy = \alpha^2 \int_{y_1}^{y_2} \{M^2(\bar{u}-c_r)^2 - 1\}(\bar{u}-c_r)^{-2} |\hat{\pi}|^2 dy, \tag{10}$$

where y_1 and/or y_2 may be at infinity. It follows from (10) that stable waves, whose relative phase speed $(c_r - \bar{u})$ is everywhere subsonic, cannot exist. However, waves whose relative phase velocity is supersonic everywhere can occur. These stable oscillations are progressive sound waves satisfying

$$\left.\begin{aligned} c_r &> \bar{u}_{\max} + M^{-1}, \\ c_r &< \bar{u}_{\min} - M^{-1}, \end{aligned}\right\} \tag{11}$$

where $\bar{u}_{\max}$ and $\bar{u}_{\min}$ denote the maximum and minimum values of $\bar{u}$ respectively. The possible existence of stable waves, which are both subsonic and supersonic over the region of flow, is not precluded by (10). In order to establish that waves of this type do exist, we shall investigate solutions of (3) with

$$\bar{u} = \operatorname{sech} y \quad (-\infty \leqslant y \leqslant \infty). \tag{12}$$

For simplicity, we shall refer to these solutions as 'stable' waves, to distinguish them from the neutrally stable waves defined by (8).

A stable solution of (3), found by inspection is,

$$\hat{\pi} = \operatorname{sech} y \tanh y, \tag{13}$$

where

$$\alpha = 2^{\frac{1}{2}}, \quad M = 1, \quad c_r = -2^{-\frac{1}{2}}. \tag{14}$$

The velocity perturbations are

$$\hat{v} = 2i\alpha^{-1} \operatorname{sech} y(\operatorname{sech} y + c_r), \tag{15}$$

$$\hat{u} = \operatorname{sech} y(\operatorname{sech} y + 2c_r) \tanh y. \tag{16}$$

The relative phase velocity of this stable wave is supersonic in the vicinity of the jet axis, ultimately becoming subsonic when $\bar{u} < 1 + c_r = 0{\cdot}293$.

In order to explore further solutions of (3), we let

$$\hat{\pi} = \bar{u}\phi, \tag{17}$$

where $\bar{u}$ is given by (12) and $c_r = c_i = 0$. Then the transformation

$$z = \tanh y \tag{18}$$

casts (3) into the form of Legendre's equation

$$(1-z^2)\phi_{zz} - 2z\phi_z + \{\nu(\nu+1) - \mu^2(1-z^2)^{-1}\}\phi = 0, \tag{19}$$

where

$$\left.\begin{aligned} \nu(\nu+1) &= (\alpha M)^2, \\ \mu^2 &= 1+\alpha^2. \end{aligned}\right\} \tag{20}$$

The boundary conditions (6) can only be satisfied if μ is an integer (Erdelyi *et al.* 1953). There are an infinite number of discrete eigenvalues and corresponding eigenfunctions, which satisfy (19) and (20). A few of the lower modes, for integer values of ν, are displayed in table 1. The perturbation velocity components may be determined from (5).

Eigenvalues			Eigenfunctions
c_r	α	M	$\hat{\pi}$
0	$3^{\frac{1}{2}}$	$2^{\frac{1}{2}}$	$\operatorname{sech}^3 y$
0	$3^{\frac{1}{2}}$	2	$\operatorname{sech}^3 y \tanh y$
0	$2(2)^{\frac{1}{2}}$	$(3/2)^{\frac{1}{2}}$	$\operatorname{sech}^4 y$
0	$2(2)^{\frac{1}{2}}$	$(5/2)^{\frac{1}{2}}$	$\operatorname{sech}^4 y \tanh y$

TABLE 1

These stable waves, like (13), are supersonic in the vicinity of the jet axis and become subsonic as $\bar{u}$ decreases. Note that both integrals in (10) remain finite because the integrands approach zero as $y \to \pm\infty$, even though $\bar{u} \to 0$.

A neutrally stable wave

When the basic flow is symmetric and $M = 0$, both symmetric and antisymmetric eigenfunctions may be found. However, they have different eigenvalues c for each α. Moreover, the first symmetric mode of the transverse velocity component $\hat{v}$, is more unstable than any $\hat{v}$ antisymmetric mode of a given basic flow (e.g. Drazin & Howard 1966). By example, we shall show that this result may be extended to include subsonic disturbances for which $M \neq 0$.

We now turn our attention to the class of waves defined by (8). We seek both symmetric and antisymmetric neutrally stable eigenfunctions associated with the basic flow (12). The numerical procedure for the determination of these

functions is discussed in § 4. However, a symmetric analytical solution corresponding to one set of eigenvalues (α_s, M, c_r) was found by inspection. This solution is

$$\hat{v} = iA \operatorname{sech} y(\operatorname{sech} y + c_r), \tag{21}$$

$$\hat{u} = \alpha_s^{-1} A \operatorname{sech} y(\operatorname{sech} y + 2c_r) \tanh y, \tag{22}$$

$$\hat{\pi} = \alpha_s^{-1} A \operatorname{sech} y \tanh y, \tag{23}$$

$$\alpha_s = 2^{\frac{1}{2}}, \quad M = 1, \quad c_r = \bar{u}_s = 2^{-\frac{1}{2}}, \tag{24}$$

where A is an arbitrary constant to be specified. Interestingly the realization of this solution led to the discovery of the stable solution (13)–(16).

4. Numerical computations

Neutral solutions

The determination of the stability characteristics of the hyperbolic-secant profile (12), as well as the normalization of the eigenfunctions, proceeded as in I.

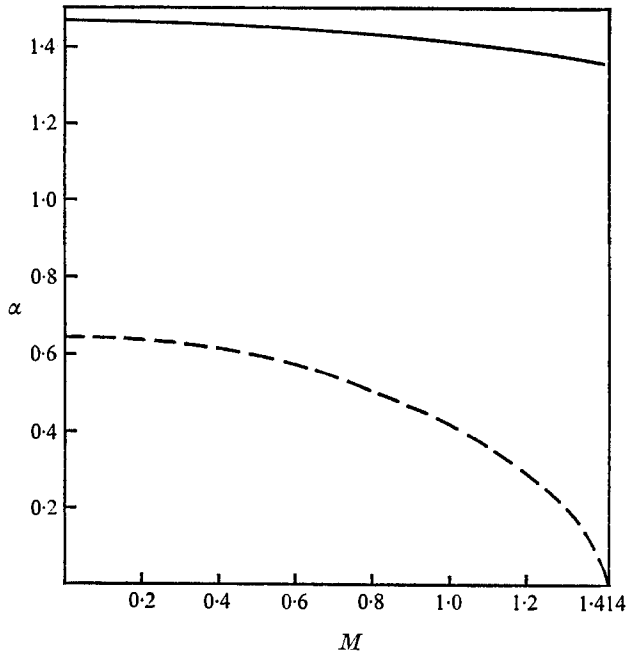

FIGURE 1. Stability boundaries for the symmetric (solid) and antisymmetric (dashed) modes.

The neutral wave characteristics are displayed in figures 1, 2 and 3 and table 2. As shown by (8), the neutral phase speed is

$$c_r = \bar{u}_s = 2^{-\frac{1}{2}} \tag{25}$$

when the basic flow is represented by (12). Thus the waves are subsonic relative to the flow at infinity if $M < 2^{\frac{1}{2}}$. It was not feasible to carry out numerical computations of eigenvalues associated with the symmetric disturbances when

$1{\cdot}4 < M < 2\frac{1}{2}$, because $\alpha(M)$ is extremely sensitive to changes in M in this range. (We do not consider the stability properties of the flow to sonic or supersonic disturbances, $M \geqslant 0$, here.) To establish whether this behaviour was due to an

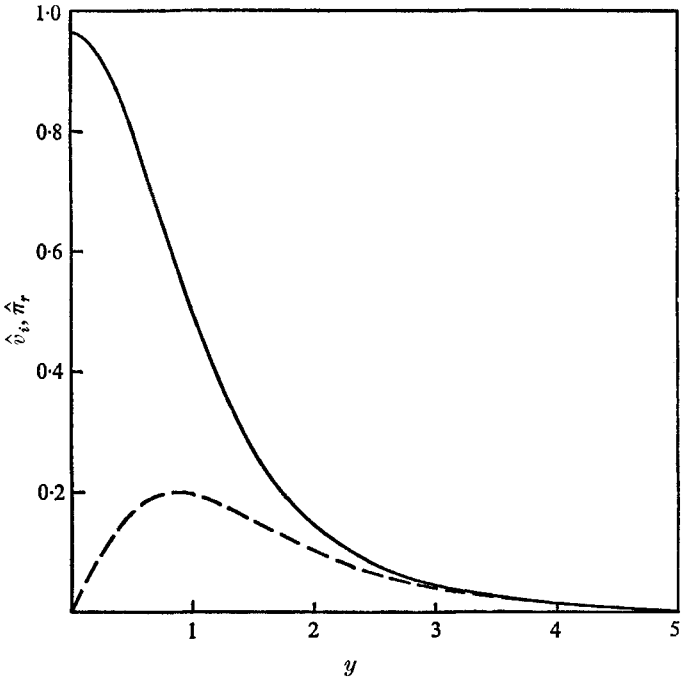

FIGURE 2. Neutral symmetric eigenfunction $\hat{v}_i$ (solid) and associated value of $\hat{\pi}_r$ (dashed) for $M = 1$. The neutral eigenfunctions for $M = 0$ and $M = 1{\cdot}4$ differ little from the functions displayed.

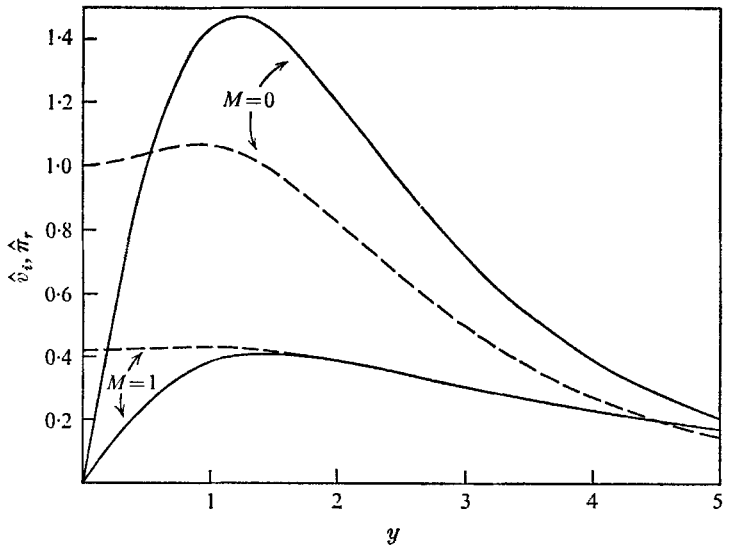

FIGURE 3. Neutral antisymmetric eigenfunctions $\hat{v}_i$ (solid) and associated values of $\hat{\pi}_r$ (dashed) for $M = 0$ and $M = 1$.

error in the numerical program, the following checks were considered: (i) The program could reproduce the analytically determined eigenvalues (24) to any accuracy desired. (ii) Computations with non-zero $c_i > 0$ showed that the neutral eigenvalues were approached smoothly as c_i was decreased down to $c_i = 10^{-5}$. Furthermore, for any M, the first symmetric mode is more unstable than any

M	Symmetric mode α_s	Antisymmetric mode α_s
0·0	1·4653	0·646
0·1	1·465	0·64
0·2	1·463	0·63
0·3	1·461	0·62
0·4	1·457	0·61
0·5	1·453	0·59
0·6	1·447	0·57
0·7	1·440	0·54
0·8	1·433	0·50
0·9	1·424	0·46
1·0	1·414	0·419
1·1	1·403	0·36
1·2	1·391	0·29
1·3	1·378	0·21
1·35	1·370	0·15
1·40	1·362	—

TABLE 2. Neutral eigenvalues

antisymmetric mode. (iii) The eigenfunctions, shown in figure 2, were determined from (4) in the range $0 \leqslant y \leqslant 8$. In order to ensure that these functions decrease in amplitude rapidly as $|y|$ increases, as required by (6), it was necessary to obtain at least three decimal place accuracy in the computed eigenvalues. Otherwise, accumulated round-off errors would at times cause the amplitudes to begin increasing slightly at some point $y \geqslant 5$. This independent check on the computed eigenvalues seems to establish their accuracy. The neutral antisymmetric eigenvalues and eigenfunctions were also checked for error by the methods employed in (ii) and (iii) above.

Unstable solutions and Reynolds stress

Unstable eigenvalues, associated with both the symmetric and antisymmetric modes, appear in tables 3 and 4. Some unstable eigenfunctions are displayed in figures 4 and 5. The initial value of the Reynolds stress, averaged over one wavelength,

$$\tau = -\overline{\mathrm{Re}\, u . \mathrm{Re}\, v} = -\tfrac{1}{2}(\hat{u}_r \hat{v}_r + \hat{u}_i \hat{v}_i) \tag{26}$$

is displayed in figure 6. The maxima of $|\tau|$ always occur at the $|y|$ associated with the inflexion points in the profile, $|y_s| = 0{\cdot}88$. These computations were made with $\Delta y = 0{\cdot}02$ and there was no evidence of jumps in τ or its derivatives in $0 \leqslant |y| \leqslant 8$. The perturbation energy equation, derived in I, may be written

$$\frac{\partial}{\partial t}\iint \epsilon \, dx\, dy = \iint \tau \bar{u}' \, dx\, dy, \tag{27}$$

where

$$\epsilon = \tfrac{1}{2}(u^2 + v^2 + M^2\pi^2) \tag{28}$$

denotes the disturbance kinetic plus elastic energy per unit mass. Since

$$\bar{u}' = -\operatorname{sech} y \tanh y,$$

an initial conversion of mean flow energy to perturbation energy occurs at all points in $0 \leqslant |y| \leqslant 8$.

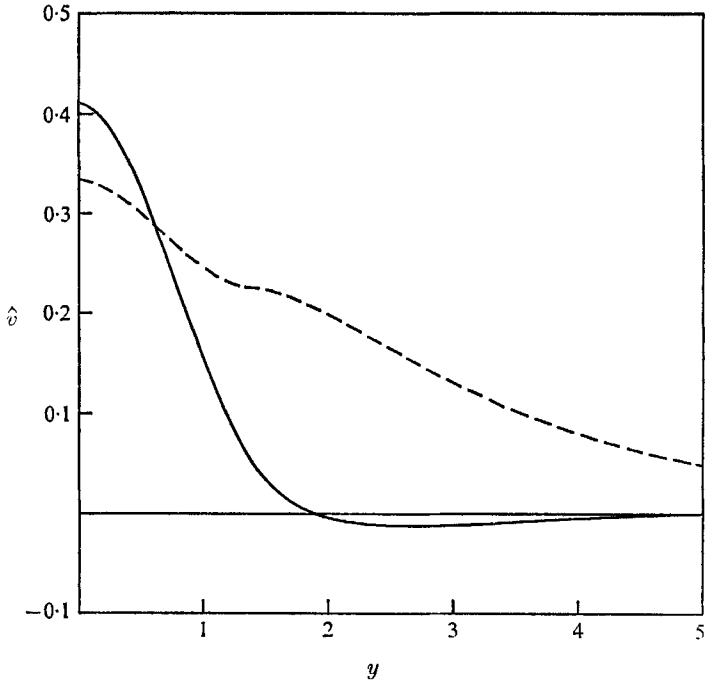

FIGURE 4. The real (dashed) and imaginary (solid) parts of the unstable symmetric eigenfunction $\hat{v}$ for $M = 1$, $\alpha = 0{\cdot}6$.

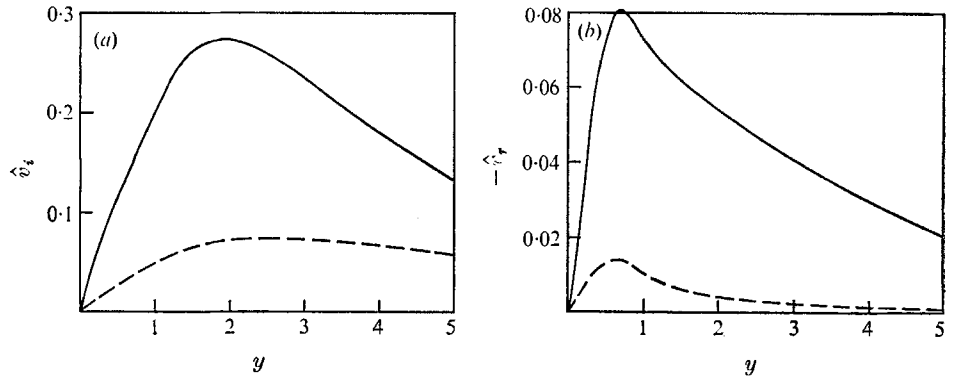

FIGURE 5. The real and imaginary parts of the unstable antisymmetric eigenfunction $\hat{v}$ for $M = 0$, $\alpha = 0{\cdot}32$ (solid) and $M = 1$, $\alpha = 0{\cdot}20$ (dashed).

	$M = 0$			$M = 1$		
α	c_r	c_i	αc_i	c_r	c_i	αc_i
1·465	0·707	0·0	0·0	—	—	—
1·414	—	—	—	0·707	0·0	0·0
1·4	0·693	0·008	0·011	0·704	0·001	0·001
1·2	0·648	0·037	0·044	0·659	0·027	0·032
1·0	0·598	0·073	0·073	0·609	0·059	0·059
0·8	0·539	0·117	0·094	0·549	0·100	0·080
0·6	0·468	0·168	0·101	0·478	0·150	0·090
0·4	0·375	0·221	0·088	0·386	0·205	0·082
0·2	0·239	0·255	0·051	0·248	0·248	0·050
0·1	0·138	0·235	0·024	0·144	0·234	0·023
0·01	0·016	0·097	0·001	0·016	0·097	0·001

TABLE 3. Unstable eigenvalues: symmetric mode

	$M = 0$			$M = 1$		
α	c_r	c_i	αc_i	c_r	c_i	αc_i
0·646	0·707	0·0	0·0	—	—	—
0·6	0·708	0·011	0·007	—	—	—
0·5	0·715	0·035	0·018	—	—	—
0·419	—	—	—	0·707	0·0	0·0
0·4	0·729	0·060	0·024	0·708	0·005	0·002
0·32	0·748	0·080	0·026	—	—	—
0·3	0·754	0·085	0·026	0·720	0·032	0·010
0·2	0·795	0·104	0·021	0·747	0·061	0·012
0·1	0·863	0·106	0·011	0·804	0·084	0·008
0·01	0·973	0·038	0·000	0·936	0·051	0·001

TABLE 4. Unstable eigenvalues: antisymmetric mode

5. Remarks

The jump in $d\tau/dy$, found in I, does not appear in the present results. However, the possibility that τ could behave differently in unexplored regions of the unstable part of the α, M plane cannot be excluded.

The symmetric mode, associated with the hyperbolic-secant profile, is able to draw upon basic flow energy in a very efficient manner since the stability characteristics of this mode are relatively insensitive to compressibility. Apparently little energy is needed to do work against the elastic force, associated with the medium, before instability is initiated. This feature is evident in figure 1 and in table 3, where the growth rates are displayed. However, the stabilizing effect of compressibility is much more in evidence when the stability characteristics of the asymmetric modes are viewed. This is also true of the unstable modes associated with the hyperbolic-tangent profile, presented in I.

The instability characteristics of the Bickley jet, presented by Drazin & Howard (1966), have been used to construct the growth rate curves in figure 7. In comparison with the present results, the Bickley jet is generally more unstable

on two counts: The instability occurs over a wider range of wave-numbers and the growth rates are larger when $\alpha \geqslant 0{\cdot}2$.

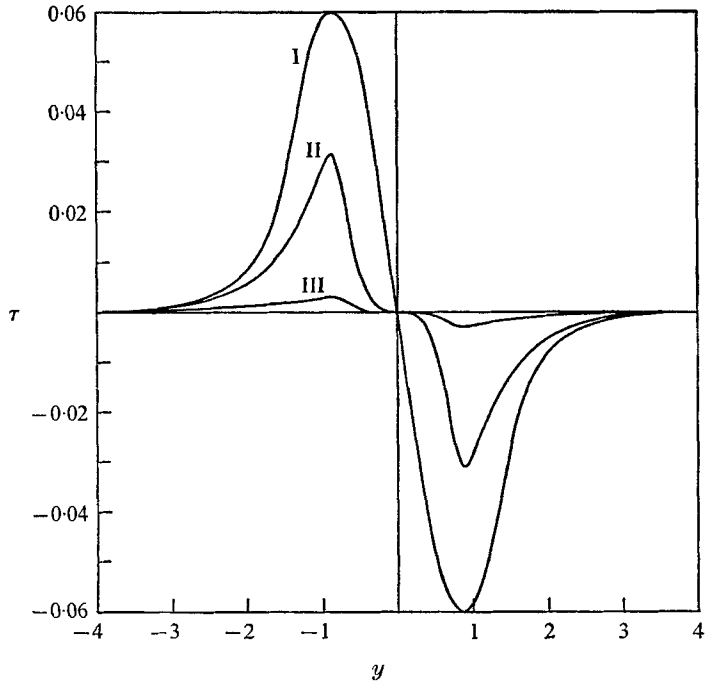

FIGURE 6. The Reynolds stress distribution associated with the symmetric mode for $M = 1$, $\alpha = 0{\cdot}6$ (I), the antisymmetric mode for $M = 0, \alpha = 0{\cdot}32$ (II) and the antisymmetric mode for $M = 1$, $\alpha = 0{\cdot}20$ (III).

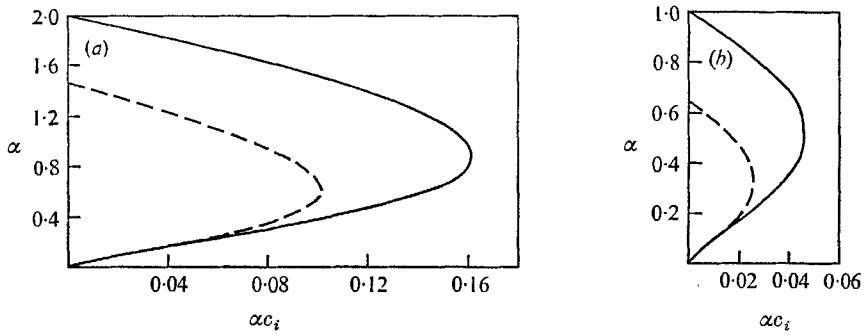

FIGURE 7. Growth rates for $M = 0$, associated with the symmetric (left) and antisymmetric (right) modes of the Bickley jet (solid) and hyperbolic-secant profile (dashed).

This research was supported by the Atmospheric Science Section of the National Science Foundation, under Grant GA-1483. Acknowledgement is also made to the National Center for Atmospheric Research, which is sponsored by the National Science Foundation, for use of its Control Data 6600 computer. All the numerical computations were programmed by Patrick J. Kennedy, to whom I am extremely grateful.

REFERENCES

BLUMEN, W. 1970 Shear layer instability of an inviscid compressible fluid. *J. Fluid Mech.* **40**, 769–81.

DRAZIN, P. G. & HOWARD, L. N. 1966 Hydrodynamic stability of parallel flow of inviscid fluid. *Advances in Applied Mechanics*, vol. 9. Academic.

ERDELYI, A., MAGNUS, W., OBERHETTINGER, F. & TRICOMI, F. G. 1953 *Higher Transcendental Functions*, vol. I, chapter III. Bateman Manuscript Project. McGraw Hill.

LEES, L. & LIN, C. C. 1946 Investigation of the stability of the laminar boundary layer in a compressible fluid. *NACA TN*, no. 1115.